**Article ID:** 1003－6326(2004)05－0952－05

# Microstructure and transformation behavior of $Ni_{50}Ti_{45}Ta_5$ shape memory alloy①

GONG Chang-wei(宫长伟), WANG Yi-nong(王轶农), YANG Da-zhi(杨大智)
(Department of Materials Engineering, Dalian University of Technology, Dalian 116024, China)

**Abstract:** The microstructure and transformation behavior of $Ni_{50}Ti_{45}Ta_5$ shape memory alloy were investigated using optical microscope, EPMA, X-ray diffraction and DSC methods. The microstructures are primary NiTi dendrite and net-like eutectic. The room temperature phases of this alloy are B2 austenite with lattice parameter $a$= 0.302 5 nm, B19′ martensite with lattice parameters $a$= 0.290 nm, $b$= 0.412 nm and $c$= 0.473 nm, β= 98.2° and a body center cubic β-Ta with lattice parameter $a'$ = 0.330 4 nm. A maximal shape memory recovery strain of 5.6% is obtained after deformation to 6.4%. The reverse transformation temperatures increase and the forward transformation temperatures decrease in the first heating/cooling cycle after deformation. The reverse transformation heat also increases with increasing deformation. The phenomenon disappears in the second heating/cooling cycle. It is closely related to the variation of elastic energy and irreversible energies during deformation.

**Key words:** microstructure; transformation behavior; $Ni_{50}Ti_{45}Ta_5$ shape memory alloy; deformation
**CLC number:** TG 139.6 **Document code:** A

## 1 INTRODUCTION

The NiTi shape memory alloy (SMA) is currently a topic of notable interest in medicine. It provides a unique opportunity to make novel surgical implants and instruments for minimally invasive, vascular and orthopedic surgery. Recently, NiTi implants have been developed for cardiovascular and gastrointestinal surgery[1-3]. The high nickel content of NiTi (54% by mass) can cause problems in biocompatibility because of toxic effects of nickel[4]. Moreover, the low X-ray visibility of NiTi SMA has limited some medical applications. Thus it is necessary to add a third element to enhance the X-ray visibility and reduce the toxic risk. It is well known that tantalum (Ta) is often used as artificial heart valves, knees, hip-joint prosthesis, and other artificial organs because of its high X-ray visibility and excellent biocompatibility. So Ta is a primary candidate.

With a proper composition, ternary Ni-Ti-Ta SMA exhibits an increased X-ray visibility[5, 6]. At the same time, the transformation temperatures of Ni-Ti-Ta alloy are less sensitive to the Ni content[5]. These features make it very attractive to biomedical application. It has been confirmed that the transformation behavior of NiTi-based alloys can be affected by various thermo-mechanical treatments, such as annealing after cold working[7], thermal cycling[8, 9], and predeformation[10-12]. This paper investigates the transformation behavior and microstructure of the $Ni_{50}Ti_{45}Ta_5$ SMA.

## 2 EXPERIMENTAL

The $Ni_{50}Ti_{45}Ta_5$ (mole fraction, %) SMA was melted in a high frequency vacuum induced furnace with CaO crucible. To improve the metallurgy quality, the master alloy $Ni_{50.8}Ti_{49.2}$ (mole fraction, %) was used. At the same time, 99.8% (mass fraction) Ta plate, 99.9% (mass fraction) electrolytic Ni plate, 99.7% (mass fraction) sponge Ti were used as raw materials. Microstructure was examined by means of MeF3 type optical microscope, EPMA-1600 type EPMA and XRD-6000 type X-ray diffraction. The specimens were cut from the ingots and mechanically polished, etched with the solution of $V(HF)$∶ $V(HNO_3)$∶ $V(H_2O)$ = 1∶ 4∶ 5. Then, the ingots were homogenized, forged, and hot drawn to 2 mm in diameter. The specimens for tensile tests were annealed for 20 min in a vacuum of $10^{-3}$ Pa at 1 123 K, followed by air-cooling and then immerged into liquid nitrogen. The tensile tests were carried out on a Schenck Test System with a rate of $4.17 \times 10^{-4}$ $s^{-1}$ at room temperature. The phase transformation temperatures were measured by differential scanning calorimetry (DSC) using a Mettler Toledo DSC822$^e$ with a heating/cooling rate of 5 K/min. The temperature running range was from 273 K to 443 K.

① **Foundation item:** Project (50171015) supported by the National Natural Science Foundation of China
**Received date:** 2004－01－05; **Accepted date:** 2004－04－23
**Correspondence:** GONG Chang-wei, PhD candidate; Tel: +86-411-84708441; E-mail: cw_gong@sina.com

## 3 RESULTS AND DISCUSSION

Fig. 1 shows the optical micrograph of as-cast $Ni_{50}Ti_{45}Ta_5$ SMA. As shown in Fig. 1, the microstructure is composed of primary NiTi dendrite and net-like eutectic. The light region labeled A represents the NiTi phase while the dark region labeled B represents the eutectic structure. The EPMA analysis shows that the constitution of the eutectic structure is NiTi phase and Ta-rich phase (Table 1).

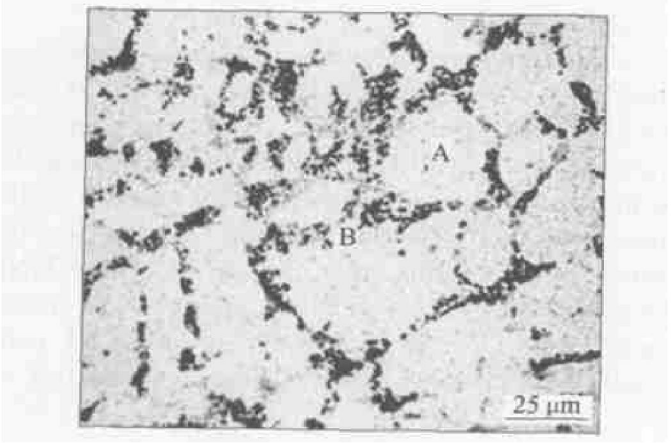


**Fig. 1** Optical micrograph of as-cast $Ni_{50}Ti_{45}Ta_5$ SMA

To identify the structure of each phase that appeared in microstructure, X-ray diffraction measurement was carried out at room temperature. Fig. 2 shows the X-ray diffraction spectrum of $Ni_{50}Ti_{45}Ta_5$ SMA. The result indicates that the room temperature phases of this alloy are B2 austenite with lattice parameter $a$ = 0.302 5 nm, B19′ martensite with lattice parameters $a$ = 0.290 nm, $b$ = 0.412 nm and $c$ = 0.473 nm, β = 98.2° and a body center cubic β-Ta with lattice parameter $a'$ = 0.330 4 nm. The lattice parameters of both B2 and B19′ are bigger than that of binary NiTi[13], because the atom radium of Ta ($r$ = 0.149 nm) is bigger than that of Ni ($r$ = 0.124 nm) and Ti ($r$ = 0.147 nm). While the lattice parameter of β-Ta is smaller than that of pure Ta ($a'_0$ = 0.330 5 nm), because β-Ta phase solutes some of Ti and Ni.

**Table 1** Results of EPMA composition analysis (mole fraction, %)

| Phase | Ni | Ti | Ta |
|---|---|---|---|
| NiTi | 51.391 | 45.144 | 3.466 |
| Ta-rich | 10.016 | 12.432 | 77.552 |

Fig. 3 shows the typical DSC curve of the $Ni_{50}Ti_{45}Ta_5$ alloy, where the upper line represents the exothermal curve and the lower the endothermic one. It can be seen that only one peak appears

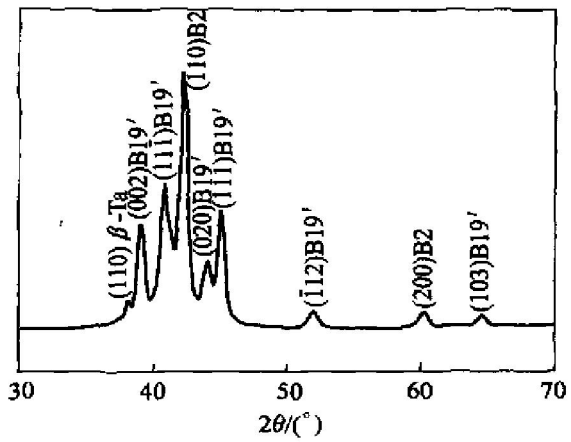


**Fig. 2** XRD pattern of cast $Ni_{50}Ti_{45}Ta_5$ alloy

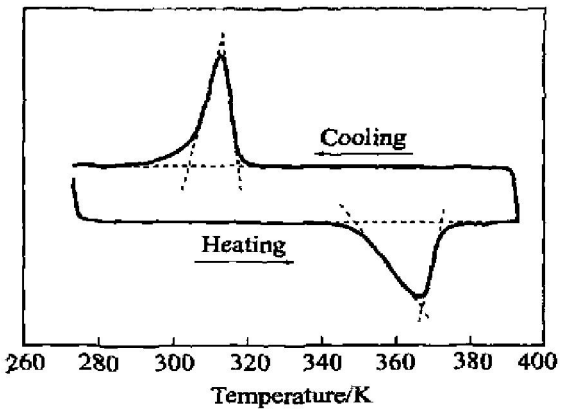


**Fig. 3** DSC curve of undeformed $Ni_{50}Ti_{45}Ta_5$ alloy

in both the forward and reverse transformation. This indicates that the phase transformation is B2 ↔ B19′ one-step transformation, no R phase transformation occurs. The martensitic transformation start temperature ($M_s$), martensitic transformation finish temperature ($M_f$), austenitic transformation start temperature ($A_s$), austenitic transformation finish temperature ($A_f$), determined using the tangent method, are 317 K, 304 K, 349 K and 372 K, respectively. Though $M_f$ is above room temperature, the martensite transformation is not completely finished at room temperature, which can be seen in Fig. 3. In other words, the B2 → B19′ transformation occurs at room temperature. The XRD result in Fig. 2 also indicates this fact.

Fig. 4 shows the shape memory effects of $Ni_{50}Ti_{45}Ta_5$ alloy deformed at room temperature. If the deformation was not more than 4.7%, the deformation could be recovered by following heating from 273 K to 443 K. The maximal recovery strain of 5.6% was obtained with a total strain of 6.4% in $Ni_{50}Ti_{45}Ta_5$ alloy. DSC curves of all specimens during the cycles of the first heating, the first cooling, the second heating and the second cooling are shown in Fig. 5. It is seen that the reverse transformation temperatures increase progressively with increasing defor-

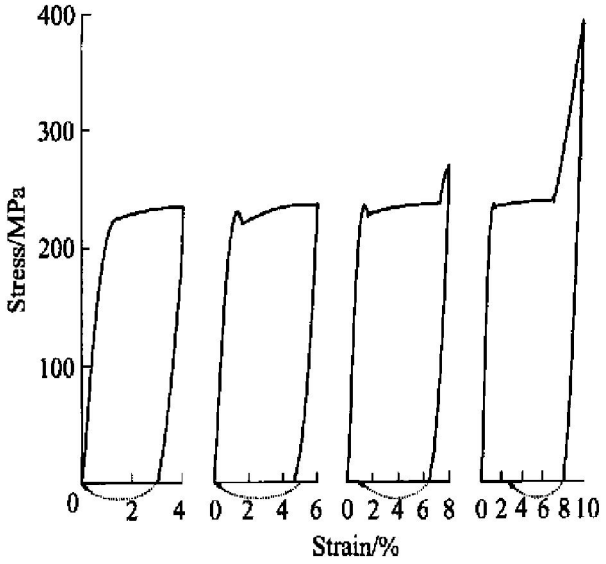


**Fig. 4** Shape memory effects of $Ni_{50}Ti_{45}Ta_5$ alloy

mation level in the first heating (Fig. 5(a)), whereas the forward transformation shifts gradually to lower temperature with increasing deformation level in the first cooling (Fig. 5(b)). However, in the second heating or cooling, the forward and reverse transformation temperatures have no obvious change with increasing the deformation level (Fig. 5(c) and 5(d)). Fig. 6 shows obviously the influence of deformation on transformation peak temperatures. In Fig. 6, $T_{A1}$ and $T_{A2}$ represent the reverse transformation peak temperatures in the first and second heating, while $T_{M1}$ and $T_{M2}$ represent the forward transformation peak temperatures in the first and second cooling, respectively. For the deformation 8.1% specimen, the $T_{A1}$ increases about 40 K, while the $T_{M1}$ decreases only about 15 K, comparing with the transformation temperature of undeformed specimen.

The transformation heat of reverse martensitic transformation versus deformation in the first heating cycle is shown in Fig. 7. We can see that the transformation heat increases with increasing deformation. It is indicated that the variation of the thermal enthalpy is the main factor affecting the transformation temperatures of the deformed TiNiTa alloy. This agrees with the result in the literatures[11,12]. The phenomenon is a result of martensite stabilization effect. This stabilization of

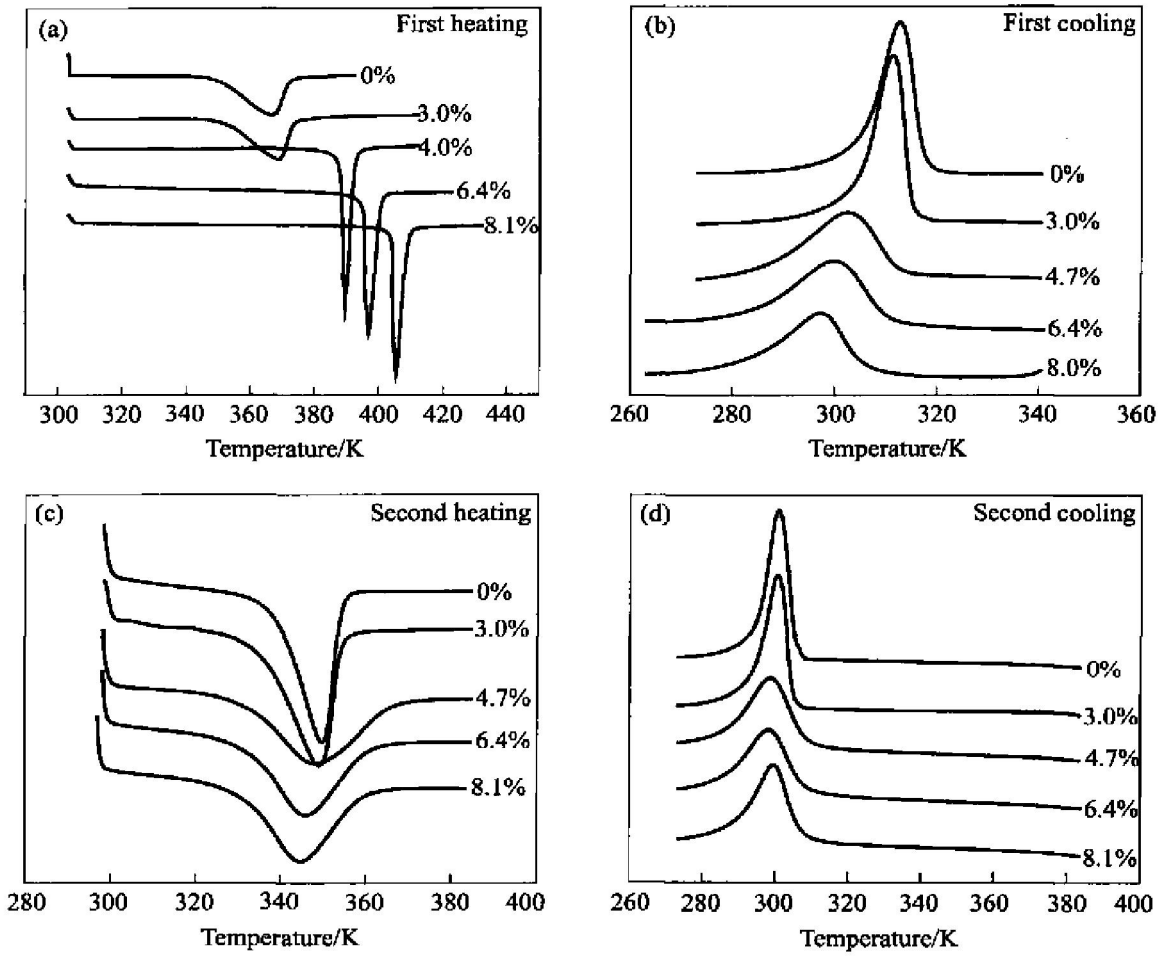


**Fig. 5** DSC curves of $Ni_{50}Ti_{45}Ta_5$ alloy after deformation
(a)—First heating; (b)—First cooling; (c)—Second heating; (d)—Second cooling

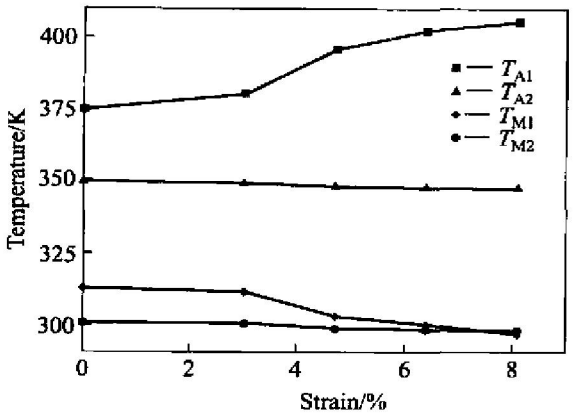


**Fig. 6** Influence of deformation on transformation temperatures

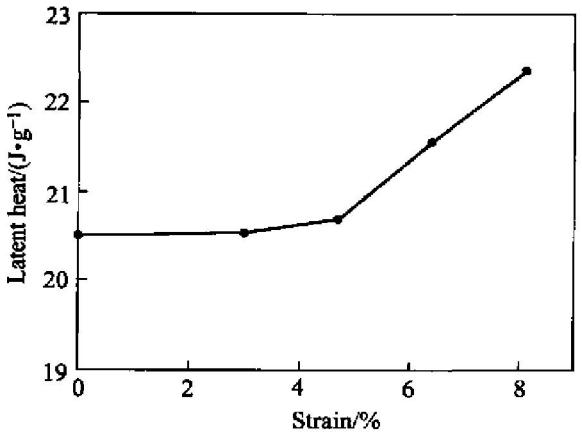


**Fig. 7** Relationship between deformation and transformation heat of reverse transformation in first heating

martensite is mainly attributed to the variation in the elastic and irreversible energies caused by deformation. The elastic energy is the drive force of the reverse transformation, while the irreversible energies are contributed to the forward transformation. The elastic energy is closely related to the structure of the martensite variants[10]. From Fig. 3, we know that the specimens after immerging into liquid nitrogen are in martensitic state at room temperature. When the samples are deformed, deformation proceeds via rearrangement of martensite variants in our study range. Since the release of elastic stain energy is related to the rearrangement of martensite variants during deformation, it can be inferred that the elastic strain energy is released as much as possible at the end of the rearrangement process. The release of the elastic strain energy results in the increase of the transformation heat thus induces the martensitic stabilization. In addition to elastic energy, the irreversible energy, which is resulted from interface plastic deformation, is also a factor of martensitic stabilization. The shape of specimen is recovered during the transformation from reoriented matensite to parent phase. More energy is needed to overcome the hindering of the interface movement because of deformation. As a result, the reverse transformation occurs at higher temperature.

For the forward transformation, $T_{M1}$ decreases as the deformation increases. This is related to the interface plastic deformation. The forward transformation is a course of growth and movement of martenstic plates. The dislocation can hinder the transformation[14, 15]. Comparing to the undeformed specimen, the dislocation around the interface can hinder the growth of martensite plates, therefore delay the forward transformation and make the $T_{M1}$ decrease.

## 4 CONCLUSIONS

1) The microstructure of the $Ni_{50}Ti_{45}Ta_5$ SMA is primary NiTi dendrite and net-like eutectic. NiTi and β-Ta make up of the net-like eutectic. The room temperature phases of this alloy are B2 austenite with lattice parameter $a$ = 0.302 5 nm, B19′ martensite with lattice parameters $a$ = 0.290 nm, $b$ = 0.412 nm and $c$ = 0.473 nm, β = 98.2° and a body center cubic β-Ta with lattice parameter $a'$ = 0.330 4 nm.

2) The maximal shape memory recovery strain is 5.6% after deformation 6.4%. Deformation via martensite reorientation causes an increase for the reverse transformation temperatures and a decrease for the forward transformation temperatures in the first heating/cooling cycle. Transformation heat also increases with increasing deformation. The phenomenon mentioned above disappears in the second cycle.

## REFERENCES

[1] Cuschieri A. Variable curvature shape-memory spatula for laparoscopic surgery[J]. Surg Endosc, 1991, 5: 179 - 181.

[2] Duerig T, Pelton A, St ckel D. An overview of nitinol medical applications[J]. Materials Science and Engineering A, 1999, 273 - 275: 149 - 160.

[3] Duerig T W, Tolomeo D E, Wholey M. An overview of superelastic stent design[J]. Min Invas Ther & Allied Technol, 2000, 9(3/4): 235 - 246.

[4] Gerber H, Perren SM. Evaluation of tissue compatibility of in vitro cultures of embryonic bone[A]. Winter G D, Leray J L, de Groot K. Evaluation of Biomaterials[C]. New York: Wiley, 1980. 307 - 314.

[5] MA Jian-lu, LIU Jiang-nan, WANG Zheng-pin, et al. Effects of Ta addition on NiTi shape memory alloys[J]. J Mater Sci Technol, 2000, 16: 534 - 536.

[6] Ma J L, Wu K H. Effects of tantalum addition on transformation behavior of $(Ni_{51}Ti_{49})_{1-x}Ta_x$ and $Ni_{50}Ti_{50-y}Ta_y$ shape memory alloys[J]. Materials Science and Technology, 2000, 16: 716 - 720.

[7] Filip P, Mazanek K. Influence of work hardening and heat treatment on the substructure and deformation behavior of NiTi shape memory alloys[J]. Scr Metall Mater, 1995, 32(9): 1375 - 1381.

[8] McCormick P G, Liu Y. Thermodynamic analysis of the martensitic transformation in NiTi—Ⅱ: effect of transformation cycling [J]. Acta Metallurgica Materialia, 1994, 42(7): 2407－2413.

[9] Miyazaki S, Imai T, Igo Y, et al. Effect of cyclic deformation on the pseudoelasticity characteristics of Ni-Ti alloys[J]. Metallurgical Transactions A, 1986, 17A: 115－120.

[10] Liu Y, Van Humbeeck J. Two-way shape memory effect developed by martensite deformation in NiTi[J]. Acta Mater, 1998, 47: 199－209.

[11] ZHENG Yan-jun, CUI Li-shan, ZHANG Fan, et al. Effects of predeformation on the reverse martensitic transformation of TiNi shape memory alloy[J]. J Mater Sci Technol, 2000, 16: 611－614.

[12] Chrobak D, Morawiec H. Thermodynamic analysis of the martensite transformation in plastically deformed Ni-Ti alloy[J]. Scripta Mater, 2001, 44: 725－730.

[13] Kudoh Y, Tokonami M, Miyazaki S, et al. Crystal structure of the martensite in Ti-49.2at% Ni alloy analyzed by the single crystal X-ray diffraction method[J]. Acta Metall, 1985, 33: 2049－2056.

[14] Pelosin V, Riviere A, Effect of thermal cycling on the R-phase and martensitic transformations in a Ti-rich Ni-Ti alloy[J]. Metallurgical and Materials Transactions A, 1998, 29A: 1175－1180.

[15] Matsumoto H. Effect of transformation-induced defects in cobalt and $Ni_{48}Ti_{52}$[J]. Physica B, 2003, 334: 112－117.

**(Edited by YUAN Sai-qian)**